Chemical Science

ROYAL SOCIETY OF CHEMISTRY

EDGE ARTICLE

View Article Online
View Journal | View Issue

Cite this: *Chem. Sci.*, 2020, **11**, 8785

All publication charges for this article have been paid for by the Royal Society of Chemistry

Modulation of the lifespan of *C. elegans* by the controlled release of nitric oxide†

Dawei Jiang,‡[a] Lei Cheng,‡[c] Yudong Xue,[a] Chao Chen,[b] Chaochao Wang,[a] Guoliang Yang,[a] An Xu,*[c] Youjun Yang,*[b] Yun Gao[a] and Weian Zhang*[a]

Received 2nd December 2019
Accepted 24th July 2020

DOI: 10.1039/c9sc06072c

rsc.li/chemical-science

The frontier of nitric oxide biology has gradually shifted from mechanism elucidation to biomanipulation, *e.g.* cell-proliferation promotion, cell-apoptosis induction, and lifespan modulation. This warrants biocompatible nitric oxide (NO) donating materials, whose NO release is not only controlled by a bioorthogonal trigger, but also self-calibrated allowing real-time monitoring and hence an onset/offset of the NO release. Additionally, the dose of NO release should be facilely adjusted in a large dynamic range; flux and the dose are critical to the biological outcome of NO treatment. *Via* self-assembly of a PEGylated small-molecule NO donor, we developed novel NO-donating nanoparticles (PEG-NORM), which meet all the aforementioned criteria. We showcased that a low flux of NO induced cell proliferation, while a high flux induced cell oxidative stress and, ultimately, death. Notably, PEG-NORM was capable of efficiently modulating the lifespan of *C. elegans*. The average lifespan of *C. elegans* could be fine-tuned to be as short as 15.87 ± 0.29 days with a high dose of NO, or as long as 21.13 ± 0.41 days with a low dose of NO, compared to an average life-span of 18.87 ± 0.46 days. Thus, PEG-NORM has broad potential in cell manipulation and life-span modulation and could drive the advancement of NO biology and medicine.

Introduction

Nitric oxide (NO) donors were first used to treat hypertensive conditions in as early as the 1800s.[1–4] Elucidation of the ubiquitous and endogenous nature and facile biological functions of NO has triggered intensive efforts to use NO as a biomanipulative or therapeutic tool.[5–14] NO is also profoundly implicated in aging.[15–17] A large body of literature has firmly established that NO related oxidative damage is partly responsible for aging. Recently, Nudler *et al.*[18] reported that bacterially derived NO enhances the longevity of *C. elegans*. This is an interesting exciting discovery because it suggests that nitric oxide potentially can be used as a molecular tool to augment lifespan, in both positive and negative manners. Yet, efforts have been largely impeded by the dichotomous biological outcome of NO under seemingly identical circumstances.[19–21] Presumably, subtle variations of the environmental parameters are believed to be responsible. This warrants a robust approach to enable delicate control of biological delivery of NO.

The direct application of NO gas is not feasible due to its reactivity and aqueous solubility. The benchmark NO donors, *e.g.* nitrosothiols and NONOates, are conditional and spontaneous NO donors.[22–28] Their NO release is heavily influenced by local environment parameters such as thiols and pH, and it is not on/off-switchable when necessary.[29,30] Ideally, the NO donor is photo-triggered and photo-calibrated.[31–35] First, light is switchable, and readily renders the desired high spatiotemporal control. Further, the flux of NO release could also be attenuated by the light intensity. Second, NO release is ideally accompanied by a fluorescence turn-on, which enables real-time and high-resolution microscopic monitoring of NO release *in vitro* and *in vivo*. This information is vital to guide the onset or offset of the photo-irradiation. Small-molecule *N*-nitrosated push–pull dyes exhibit sharp onset/offset of NO release, precise dose controllable NO release, and favorable stability against biomacromolecules.[36–44] Yet, they still lack a high loading of NO to allow the NO release be adjusted in a large dynamic range for biomanipulation.

Nanotechnology has been widely utilized in biology during the past few decades, which usually can improve the water solubility of hydrophobic drugs, increase the drug loading efficiency and enhance the biocompatibility of functional small molecules.[45–51] Herein, the hydrophobic *N*-nitrosated naphthalimide was tailored with a hydrophilic poly-ethylene glycol

[a]*Shanghai Key Laboratory of Functional Materials Chemistry, School of Chemistry and Molecular Engineering, Shanghai, China. E-mail: wazhang@ecust.edu.cn*

[b]*Shanghai Key Laboratory of Chemical Biology, School of Pharmacy, East China University of Science and Technology, 130 Meilong Road, Shanghai 200237, China. E-mail: youjunyang@ecust.edu.cn*

[c]*School of Environmental Science and Optoelectronic Technology, University of Science and Technology of China, Hefei, Anhui 230026, China. E-mail: anxu@ipp.ac.cn*

† Electronic supplementary information (ESI) available. See DOI: 10.1039/c9sc06072c

‡ These authors contributed equally.

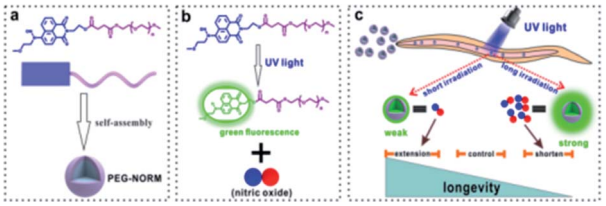

Scheme 1 (a) Schematic illustration of the formation of PEG-NORM nanoparticles. (b) The mechanism for self-calibrating the released NO. (c) Schematic illustration of modulating the longevity of the *C. elegans* by PEG-NORM nanoparticles.

(PEG) chain to enable self-assembly to form photo-calibrated, kinetics-controlled and dose-controllable NO-releasing biocompatible nanoparticles (PEG-NORM) (Scheme 1a and b). Firstly, DLS and TEM were utilized to characterize the prepared PEG-NORM nanoparticles. Then, the Griess assay was used to validate the capability of self-calibration. Subsequently, the robust control of NO release from the PEG-NORM nanoparticles was checked by manipulating the output power density, sample concentration and irradiation time. Furthermore, *in vitro* evaluation against A549 and L-02 cells was conducted by control of intracellular NO release. Finally, *in vivo* modulation of the lifespan of *C. elegans* was exemplified (Scheme 1c).

Results and discussion

NORM was conveniently prepared in three synthetic steps (Fig. 1a and S1–S6†). 4-Bromo-1,8-naphthalic anhydride (BNA) was condensed with ethanolamine, substituted with 2-methoxyethylamine and then *N*-nitrosated to prepare NO. Installation of the nitroso group is evidenced by the down-field shift of the aromatic proton at the ortho position (Fig. S4†). PEG-NORM was obtained by esterification of NORM and PEG-COOH (Fig. S7 and S8†). The gel permeation chromatography (GPC) trace of PEG-NORM shifted to the higher molecular weight region in comparison to that of PEG-COOH; furthermore, the molecular weight distribution of PEG-NORM is very low with a PDI value of

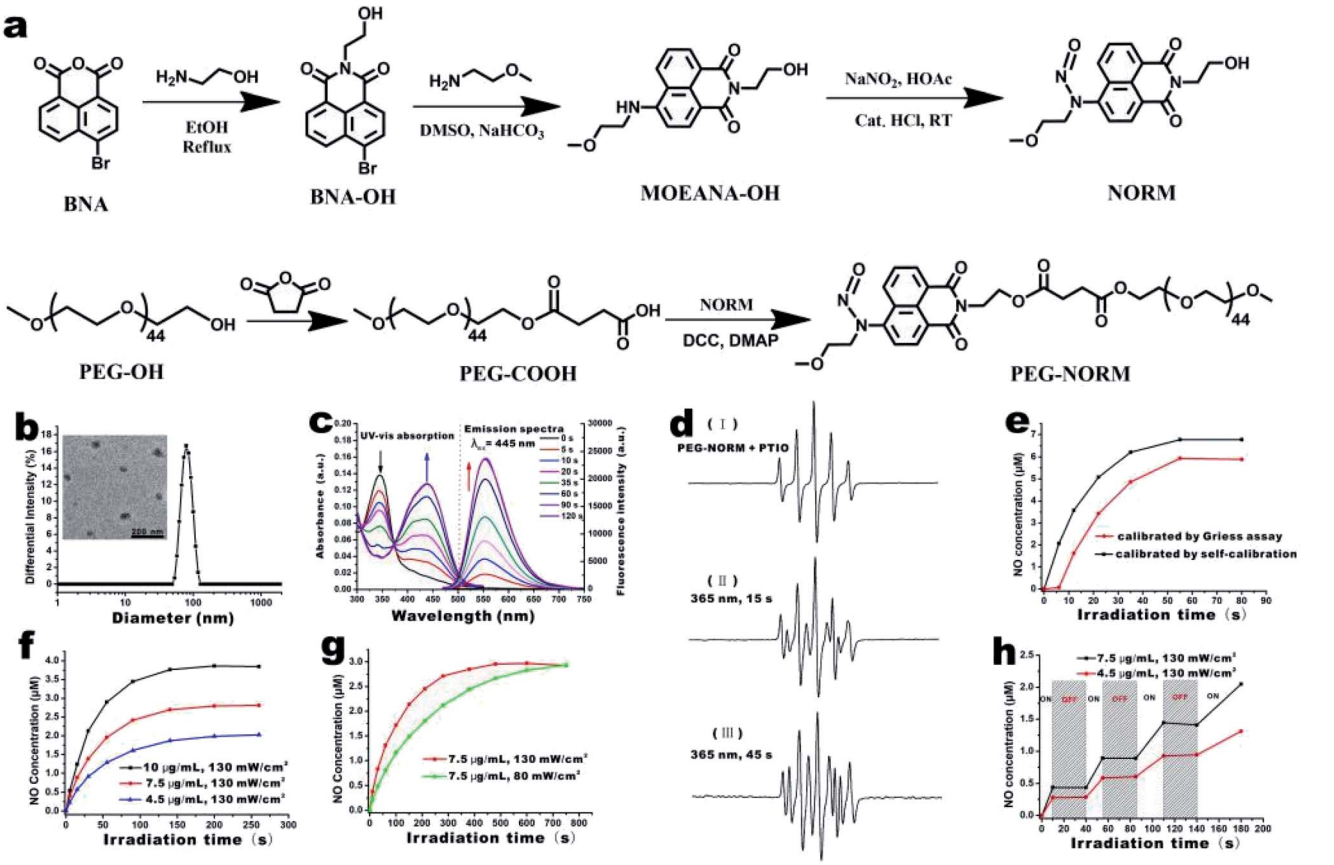

Fig. 1 (a) The synthetic route of PEG-NORM. (b) DLS and TEM images (the inset) of the PEG-NORM nanoparticles. (c) The changes of the UV-vis absorption spectra and fluorescence spectra (λ_{ex} = 445 nm) of the PEG-NORM nanoparticles irradiated with 365 nm light for different times. (d) ESR spectra of PTIO in the presence of PEG-NORM nanoparticles. Samples contained 10 μM PTIO and 20 μM PEG-NORM nanoparticles in aqueous solution; ESR spectra were recorded with a modulation amplitude of 2.0 G after photo-irradiation for 0 s, 15 s, and 45 s. (e) The NO release curve of the PEG-NORM nanoparticles simultaneously detected by self-calibration and the Griess assay in one system. (f) The NO release curve of the PEG-NORM nanoparticles with different concentrations detected by self-calibration, with the same output power (130 mW cm^{-2}). (g) The NO release curve of the PEG-NORM nanoparticles with different output power (130 mW cm^{-2} or 80 mW cm^{-2}) detected by self-calibration, but with the same sample concentration. (h) On-demand NO release by manipulating "on or off" of UV light and detected by self-calibration.

1.05 (Fig. S9†). These results clearly demonstrated that PEG-NORM was successfully synthesized.

The amphiphilic nature of PEG-NORM renders a high tendency to self-assemble in an aqueous medium. PEG-NORM (10 mg mL^{-1} in THF) was added dropwise into four volumes of deionized water under vigorous stirring. The PEG-NORM nanoparticles were observed by TEM upon removal of THF *via* dialysis. PEG-NORM was found to form spherical aggregates with a diameter of 54.3 nm in water by TEM (the inset of Fig. 1b). DLS was utilized to characterize the resulting PEG-NORM nanoparticles (Fig. 1b). The hydrodynamic diameter of the nanoparticles is measured to be *ca.* 83 nm and a polydispersity index (PDI) of 0.14 was calculated. The diameter of the PEG-NORM nanoparticles by DLS was bigger because PEG chains were solvated and therefore fully extended in aqueous solution. Furthermore, the PEG-NORM nanoparticles had good stability in PBS for at least one week (Fig. S10†).

The optical properties of PEG-NORM nanoparticles were subsequently investigated. UV light (80 mW cm^{-2} at 365 nm) irradiation of PEG-NORM nanoparticles (20 μg mL^{-1}) in H_2O led to immediate changes of the UV-vis absorption and fluorescence emission spectra. The characteristic absorption peak at 345 nm gradually reduced, meanwhile the absorption peak at 445 nm increased (Fig. 1c). At the same time, the fluorescence emission intensity at 558 nm significantly enhanced ($\lambda_{ex} = 445$ nm). It took *ca.* 90 seconds for complete decomposition of PEG-NORM nanoparticles, suggesting that the high efficiency of UV-triggered decomposition of NORM was not affected upon nanoencapsulation into a hydrophobic environment (Fig. S11 and S12†).

Since the therapeutic efficacy of NO is greatly dependent on its concentration, it is crucial to be able to sensitively and conveniently monitor the NO release from a given NO donor. Firstly, the NO release from PEG-NORM nanoparticles was checked by ESR assay with PTIO (2-phenyl-4,4,5,5,-tetramethylimidazoline-1-oxyl-3-oxide). PTIO is a persistent radical and has been routinely used as a spin trap for NO. Under irradiation with 365 nm light for 15 s, the PTIO signal varied between Fig. 1d(I) and (II). By extending the irradiation time to 45 s, the PTIO signal changed more (Fig. 1d(III)). This spectral change confirms that NO has indeed been released from PRG-NORM nanoparticles. In addition, PEG-NORM nanoparticles yield an off-on fluorescence enhancement upon photo-induced NO release (Fig. 1c), enabling a built-in self-calibration mechanism for real-time and high-resolution monitoring of the NO release. It is known that nitrite is the sole end-product of aerial oxidation of nitric oxide. Therefore, the Griess assay,[52] a commercial nitrite kit, was employed to check the accuracy and sensitivity of this built-in fluorescence-based calibration method.

An aliquot of the PEG-NORM solution was irradiated with UV light at 365 nm for different times and the fluorescence emission intensity of the resulting solution was recorded (Fig. S15†). A small amount of the resulting solution was spiked and subjected to the Griess assay for nitrite concentration (Fig. S16†). Overall, a similar trend was observed with the results from both the built-in fluoremetric method and the external Griess assay (Fig. 1e). However, a notable subtle difference exists. The fluorescence enhancement of the solution was immediately observed upon photo-irradiation. However, the Griess assay suggested negligible nitrite formation during this time period. Two factors have contributed to this discrepancy. First, the Griess assay has a lower detection limit of *ca.* 0.5 μM and the initial build-up of the nitrite lower than this level was therefore invisible in the Griess assay. Second, the aerial oxidation of NO, especially at the nM level, is so slow that nitric oxide was not converted into nitrite during the time window of the Griess assay. This is a clear indication that such a built-in fluorescence-based self-calibration mechanism is superior because of its sensitivity and feasibility for real-time monitoring of NO release.

The dose-controlled NO release is very important for biological manipulation or disease treatment. Potential options for delicate control of the NO release from the PEG-NORM nanoparticles were checked. The NO releasing profiles of the PEG-NORM nanoparticles were established harnessing the fluorimetric self-calibration mechanism. First, the NO release could be controlled by using different amounts of PEG-NORM. Solutions of PEG-NORM, containing 4.5, 7.5 and 10 μg mL^{-1} respectively, were prepared and irradiated (Fig. 1f). A higher signal enhancement was obtained with the solution containing a higher dose of the donor, under the same UV-irradiation (130 mW cm^{-2}). Second, the flux of NO release could also be regulated by manipulating the power density of the UV-light at the same concentration of the PEG-NORM nanoparticles. It took *ca.* 200 s for the solution to complete NO releasing with a 130 mW cm^{-2} UV-lamp (Fig. 1g). However, 700 s was needed if the light power density was reduced from 130 mW cm^{-2} to 80 mW cm^{-2}. Third, the NO release could be switched on or off at will, facilitating on-demand NO release. When the UV light was switched on, a burst of NO release was observed from the nanoparticles. However, the NO release completely stopped, when the UV light was switched off (Fig. 1h). These results clearly showcased the rate- and dose-controllability of PEG-NORM nanoparticles.

The existing nitric oxide fluorescent probes, such as DAF-2DA,[53] CuFL[54] and DAF-FM DA[55] have been used to monitor intracellular NO, by reacting with NO or its aerial oxidized derivative (NO+ equivalent) to produce a fluorescent molecule. However, they are not suitable for monitoring NO release from a donor, since they detect by scavenging NO and therefore prohibit NO from eliciting downstream biological activities.

The applicability of the self-calibration mechanism for monitoring NO release in *in vitro* settings was further showcased. The PEG-NORM nanoparticles were incubated with A549 cells for 24 h to facilitate cell-uptake and then the residual nanoparticles outside the cells were washed off. The A549 cells were fixed by paraformaldehyde, stained with DAPI, and imaged by using a confocal laser scanning microscope (CLSM). Without UV-irradiation, no green fluorescence in A549 cells was observed, suggesting that NO was not released from the nanoparticles (Fig. 2). Then, UV light at 365 nm was used to irradiate these A549 cells for 5 s and green fluorescence was observed from the cells, suggesting photo-induced decomposition of the PEG-NORM and release of NO. Exposure of the cells to UV light for another 5 s induced a corresponding further enhancement

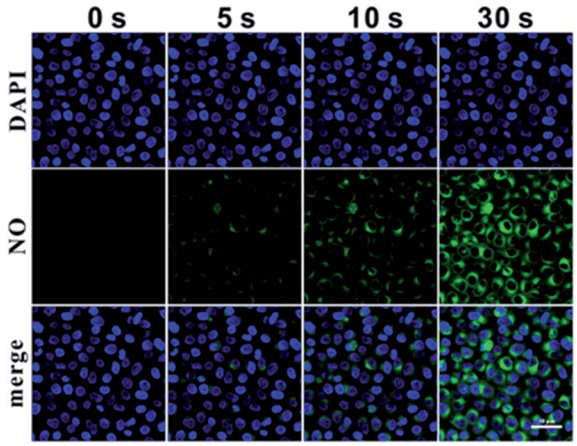

Fig. 2 Detection of intracellular NO release with self-calibration. After incubating with the PEG-NORM nanoparticles and staining with DAPI, the A549 cells were put on a CLSM and irradiated with different times (0 s, 5 s, 10 s, and 30 s). For each panel, images from up to down show cell nuclei stained by DAPI (blue), self-calibration of the released NO from the PEG-NORM nanoparticles in A549 cells (green), and overlays of the above images. All images have the same scale bar (50 μm).

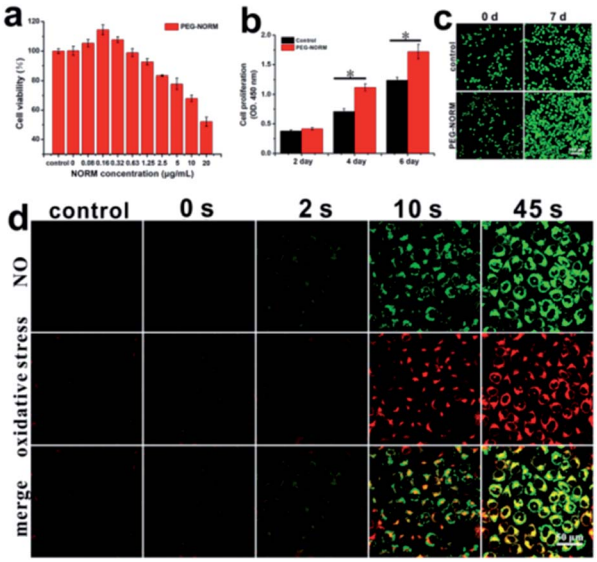

Fig. 3 (a) Cellular manipulation against A549 cells by the PEG-NORM nanoparticles, irradiated with UV light (130 mW cm^{-2}) for 45 s, detected by MTT assay. (b) Cell proliferation assay of the PEG-NORM nanoparticles, irradiated with UV light (80 mW cm^{-2}) for only 2 s, detected by CCK-8 assay. The experiments were repeated at least three times. Statistical significance was calculated using two-way analysis of variance (ANOVA), followed by the Bonferroni multiple comparison test. *, $p < 0.05$. (c) Cell proliferation assay of PEG-NORM nanoparticles detected by using a CLSM. After incubating with PEG-NORM nanoparticles for 24 h, the A549 cells were irradiated with UV light (80 mW cm^{-2}) for 2 s then cultured in an incubator for 0 d or 7 d. The A549 cells without treatment were used as a control. Before detection, the cells were stained with Calcein-AM. All images have the same scale bar (100 μm). (d) Detection of intracellular oxidative stress. After incubating with the nanoparticles and CellROX Deep Red Reagent, the A549 cells were irradiated with UV light (80 mW cm^{-2}) for different times (control, 0 s, 2 s, 10 s or 45 s). For each panel, images from up to down were self-calibration of the released NO (green), the oxidative stress detection (red) and overlays of the above images. All images have the same scale bar (50 μm).

of the green fluorescence, in agreement with our expectation. After 30 s, the green emission reached a plateau. In addition, a cell localization experiment indicated that intracellular PEG-NORM nanoparticles were localized in lysosomes (Fig. S17†). These experiments have confirmed the following three points. First, PEG-NORM nanoparticles are stable intracellularly without exposure to UV light. Second, NO release can be readily triggered by exposure to UV light whenever necessary. Third, importantly, the NO release can be conveniently followed by the fluorescence turn-on of the PEG-NORM nanoparticles.

Encouraged by the controllable NO release in A549 cells, the use of the PEG-NORM nanoparticles as a biomanipulative tool was evaluated by MTT assay. First, the dark cytotoxicity of the PEG-NORM nanoparticles was checked against A549 cells. PEG-NORM exhibited negligible cytotoxicity, tested up to 20 μg mL^{-1} since the cell viability remained 95% or higher (Fig. S18†), where the concentration (20 μg mL^{-1}) of PEG-NORM is much higher than its critical micelle concentration (CMC) in PBS.[56,57] Then, the cytotoxicity of PEG-NORM nanoparticles upon photo-irradiation was evaluated with A549 cells. Cells were incubated with the PEG-NORM nanoparticles for 24 h to facilitate cell uptake, and then irradiated with UV light (80 mW cm^{-2}) for 45 s followed by a second 24 h incubation. It is interesting to see that a low concentration of the PEG-NORM nanoparticles promoted cell proliferation as evidenced by viability higher than 100% (Fig. 3a). In particular, the cell viability was the highest at 113.6% when 0.16 μg mL^{-1} of nanoparticles was used. With an increased concentration of PEG-NORM, the cell viability started to gradually drop. When the PEG-NORM nanoparticles were at 20 μg mL^{-1}, cell viability was 51.6%. Furthermore, human L-02 hepatocytes were also utilized to *in vitro* evaluate the PEG-NORM nanoparticles, which exhibited a similar trend with A549 cells. Nitric oxide with a low concentration promoted L-02 cell proliferation, but induced obvious reduction of L-02 cell viability (Fig. S19†).

It has been acknowledged that NO at a low level promotes cell proliferation and bolus addition of NO donors induces cytotoxicity. However, to our knowledge, NO releasing materials rarely exhibited a comparable degree of facile control of cell proliferation or cell death. This clearly delineates the potential of PEG-NORM nanoparticles as a cell manipulative tool. The capability of PEG-NORM nanoparticles to induce cell proliferation was further evaluated by the CCK-8 assay.[58,59]

After a 24 h incubation with PEG-NORM nanoparticles (20 μg mL^{-1}), the residual nanoparticles outside the cells were washed off. The treated A549 cells were irradiated with UV light for a short duration of 2 s (80 mW cm^{-2}) in order to generate NO with a low concentration. As shown in Fig. 3b, the cell proliferation rate of cells treated with the PEG-NORM nanoparticles significantly enhanced compared with the control group. To further verify this phenomenon, a CLSM was utilized to image the PEG-NORM nanoparticle treated cells, which were stained with Calcein-AM before imaging. As shown in Fig. 3c, the cell density in the PEG-NORM group is obviously higher than the control group at 7 d.

The cytotoxicity of PEG-NORM nanoparticles at a high concentration has been routinely achieved. Oxidative stress from the photo-triggered release of NO is presumably the cause of cell death. Therefore, we employed CellROX Deep Red,[60,61] a fluorescent probe for oxidative stress, to confirm such a hypothesis. Prior to the UV light irradiation, the green fluorescence from the PEG-NORM nanoparticles did not appear (Fig. 3d). Correspondingly, the red fluorescence reflective of oxidative stress was exhibited, almost the same as that of the control group. Upon UV-irradiation for 2 s (80 mW cm^{-2}), NO release occurred and the green fluorescence from PEG-NORM nanoparticles was evident, but the red fluorescence from CellROX Deep Red was still negligible. This indicated that a small amount of the released NO does not lead to obvious changes of intracellular oxidative stress. By extending the illumination time to 10 s and 45 s, the green fluorescence increased remarkably and the red fluorescence intensity also obviously enhanced, suggesting the release of a large amount of NO from the nanoparticles. At the same time, the red fluorescence was significantly enhanced, indicative of an increased intracellular oxidative stress. This experiment verifies the potential of PEG-NORM to be employed as a therapeutic material. However, to our knowledge, NO releasing materials rarely exhibited a comparable degree of facile control of cell proliferation or cell death. This clearly delineates the potential of PEG-NORM nanoparticles as a cell manipulative tool.

Caenorhabditis elegans (*C. elegans*), due to their short life cycle and transparent body, have been routinely employed as a multicellular organism for microscopic evaluation of an effect of a xenophile on lifespan.[62–66] Firstly, controllable NO release in *C. elegans* from PEG-NORM nanoparticles was confirmed by its self-calibration mechanism, *i.e.* the green fluorescence emission. The PEG-NORM nanoparticles were incubated with *C. elegans* for 24 h to facilitate ingestion and then the residual nanoparticles outside the worms were washed off. Then, the *C. elegans* were imaged by using a fluorescence microscope. Without UV light-irradiation, no green fluorescence in the intestine and pharynx of *C. elegans* was observed, suggesting that NO was not released from the nanoparticles (Fig. 4a and b). Then, UV light (365 nm) was utilized to irradiate these *C. elegans* for 5 s. Meanwhile, the green fluorescence was observed from the intestines and pharynx, suggesting photo-induced decomposition of the PEG-NORM and release of NO. Exposure of the *C. elegans* to UV light for another 5 s induced a corresponding further enhancement of the green fluorescence, in agreement with our expectation. After an irradiation of 30 s, the green emission reached peak intensity. These results verified that robust control of NO release from PEG-NORM nanoparticles can be realized in *C. elegans*.

Encouraged by the controllable NO release in *C. elegans*, the *in vivo* toxicity of PEG-NORM nanoparticles against *C. elegans* was subsequently assessed by means of the endpoints of germline cell apoptosis, life-span assay, body length and brood size. First, we evaluated the germline cell apoptosis of *C. elegans*. The PEG-NORM nanoparticles (5 μg mL^{-1}) were incubated with *C. elegans* for 24 h to facilitate ingestion and the residual nanoparticles outside the worms were washed off. Then, the worms were irradiated with UV light for different durations (0 s, 1 s, 3 s, 5 s, 10 s, 30 s or 60 s, respectively) to precisely manipulate the amount of the released NO. As shown in Fig. 5, the germline cell apoptosis of *C. elegans*, irradiated with UV light (130 mW cm^{-2}) for 0 s, 1 s and 3 s, exhibited similar results to the control group, suggesting that a small amount NO release induced negligible germline cell apoptosis. However, by extending the irradiation time to 5 s, 10 s, 30 s or 60 s, the

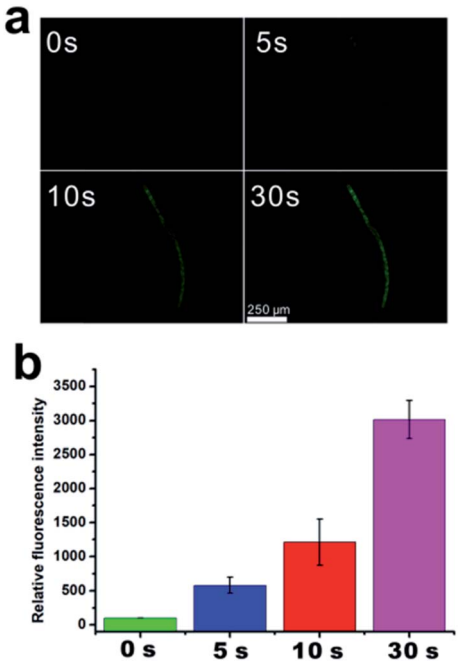

Fig. 4 (a) Detection of NO release in *C. elegans* by self-calibration. After incubating with PEG-NORM nanoparticles, the worms were put on a fluorescence microscope and irradiated with UV light for different times (0 s, 5 s, 10 s or 30 s, respectively). All images have the same scale bar (250 μm). (b) The corresponding fluorescence intensity of the *C. elegans* irradiated with 0 s, 5 s, 10 s or 30 s, respectively.

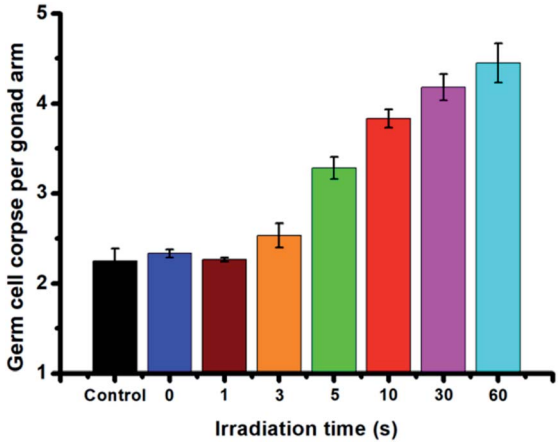

Fig. 5 Germ cell apoptosis induced by PEG-NORM nanoparticles, irradiated with UV light (130 mW cm^{-2}) for 0 s, 1 s, 3 s, 5 s, 10 s, 30 s or 60 s, respectively. The experiments were repeated three times. The *C. elegans* without any treatment was used as a control group.

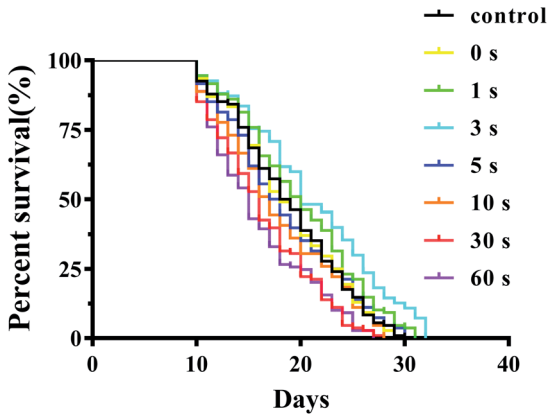

Fig. 6 Lifespan curves of PEG-NORM nanoparticle incubated worms irradiated with UV light (130 mW cm^{-2}) for 0 s, 1 s, 3 s, 5 s, 10 s, 30 s, and 60 s, respectively. More than thirty worms were scored for each group. The *C. elegans* without any treatment were used as control group.

germline cell apoptosis increased, as a result of the high dose of released NO from PEG-NORM nanoparticles.

In the life-span assay, a blank control experiment was conducted to investigate the effect of only UV light irradiation on *C. elegans*. As shown in Fig. S20 and Table S1,† the same average lifespan of the *C. elegans* irradiated with UV light for 1 s, 3 s, 5 s, 10 s, and 30 s, respectively, did not exhibit significant difference compared with the control group ($P > 0.05$). Only on extending the UV irradiation time to 60 s, the average lifespans of *C. elegans* slightly decreased. Subsequently, we investigated the influence of PEG-NORM nanoparticles on the lifespan of *C. elegans* under UV light irradiation. As expected, the PEG-NORM nanoparticles treated *C. elegans* irradiated with UV light for 30 s or 60 s had a shorter average life span compared with the control group ($P < 0.01$, Fig. 6 and Table S2†). Compared with the control group, the average lifespan of the *C. elegans* treated with PEG-NORM nanoparticles and irradiated with UV light for 60 s decreased to 15.9%, which may be mainly attributed to a large amount of NO release. In addition, it's interesting to find that the *C. elegans* treated with PEG-NORM nanoparticles and UV light irradiation for 3 s showed a significantly longer average lifespan, increased 12.00% to that of the control group ($p < 0.01$, Table S2†), indicating that a low concentration of released NO is beneficial for *C. elegans*. Although the body length irradiated with UV light for different durations exhibited negligible change (Fig. S21†), the brood size of the treated *C. elegans* has similar trends to germline cell apoptosis. The brood size of the treated *C. elegans* irradiated with UV light less than 3 s didn't show a significant change, but gradually decreased by extending the irradiation time (Fig. S22†).

Conclusions

In summary, PEG-NORM nanoparticles were successfully prepared and their potential in biomanipulation was showcased. The PEG-NORM nanoparticles are biocompatible and enable switchable release of NO *via* photo-irradiation. The flux of NO release can be facilely controlled by the intensity and duration of irradiation. The dose of NO release is conveniently and accurately monitored by a self-calibration mechanism without the necessity for external NO-probes. A low flux of nitric oxide from photoirradiation of PEG-NORM was showcased to promote A549 and L-02 cell proliferation, while a high flux induced cell oxidative stress and death. Additionally, a low dose of NO release could be physiological and promote the lifespan of *C. elegans*, while a high dose of NO elicited by extending the irradiation time is generally pathological and results in germline cell apoptosis, decrease of brood size and decline of lifespan. The robustness of PEG-NORM for on-demand NO delivery makes it an ideal candidate for modulating NO related biological processes, such as aging.

Conflicts of interest

There are no conflicts to declare.

Acknowledgements

This work was financially supported by the National Natural Science Foundation of China (21875063 and 21822805), and the Science and Technology Commission of Shanghai Municipality for the Shanghai International Cooperation Program (19440710600).

Notes and references

1 O. A. Paniagua, M. B. Bryant and J. A. Panza, *Circulation*, 2001, **103**, 1752–1758.
2 S. Ulker, D. McMaster, P. P. McKeown and U. Bayraktutan, *Cardiovasc. Res.*, 2003, **59**, 488–500.
3 H. G. Li, K. Witte, M. August, I. Brausch, U. Godtel-Armbrust, A. Habermeier, E. I. Closs, M. Oelze, T. Munzel and U. Forstermann, *J. Am. Coll. Cardiol.*, 2006, **47**, 2536–2544.
4 U. Forstermann, *Pflug. Arch. Eur. J. Phy.*, 2010, **459**, 923–939.
5 C. Bogdan, *Trends Cell Biol.*, 2001, **11**, 66–75.
6 J. A. McCleverty, *Chem. Rev.*, 2004, **104**, 403–418.
7 S. Mocellin, V. Bronte and D. Nitti, *Med. Res. Rev.*, 2007, **27**, 317–352.
8 I. D. Wilson, S. J. Neill and J. T. Hancock, *Plant Cell Environ.*, 2008, **31**, 622–631.
9 L. Wen, S. Feil, M. Wolters, M. Thunemann, F. Regler, K. Schmidt, A. Friebe, M. Olbrich, H. Langer, M. Gawaz, C. de Wit and R. Feil, *Nat. Commun.*, 2018, **9**, 4301.
10 C. Bonnet, J. Hao, N. Osorio, A. Donnet, V. Penalba, J. Ruel and P. Delmas, *Nat. Commun.*, 2019, **10**, 4253.
11 S. Hartman, Z. Liu, H. van Veen, J. Vicente, E. Reinen, S. Martopawiro, H. Zhang, N. van Dongen, F. Bosman, G. W. Bassel, E. J. W. Visser, J. Bailey-Serres, F. L. Theodoulou, K. H. Hebelstrup, D. J. Gibbs, M. J. Holdsworth, R. Sasidharan and L. A. C. J. Voesenek, *Nat. Commun.*, 2019, **10**, 4020.
12 Y. Sun, S. Chen, X. Chen, Y. Xu, S. Zhang, Q. Ouyang, G. Yang and H. Li, *Nat. Commun.*, 2019, **10**, 1323.

13 C. J. McCann, J. E. Cooper, D. Natarajan, B. Jevans, L. E. Burnett, A. J. Burns and N. Thapar, *Nat. Commun.*, 2017, **8**, 11.
14 Y. F. Miao, N. E. Ajami, T. S. Huang, F. M. Lin, C. H. Lou, Y. T. Wang, S. Li, J. Kang, H. Munkacsi, M. R. Maurya, S. Gupta, S. Chien, S. Subramaniam and Z. Chen, *Nat. Commun.*, 2018, **9**, 13.
15 S. M. McCann, *Exp. Gerontol.*, 1997, **32**, 431–440.
16 S. M. McCann, J. Licinio, M. L. Wong, W. H. Yu, S. Karanth and V. Rettorri, *Exp. Gerontol.*, 1998, **33**, 813–826.
17 S. M. McCann, C. Mastronardi, A. de Laurentiis and V. Rettori, *Ann. N. Y. Acad. Sci.*, 2005, **1057**, 64–84.
18 I. Gusarov, L. Gautier, O. Smolentseva, I. Shamovsky, S. Eremina, A. Mironov and E. Nudler, *Cell*, 2013, **152**, 818–830.
19 W. M. Xu, L. Z. Liu, M. Loizidou, M. Ahmed and I. G. Charles, *Cell Res.*, 2002, **12**, 311–320.
20 A. J. Burke, F. J. Sullivan, F. J. Giles and S. A. Glynn, *Carcinogenesis*, 2013, **34**, 503–512.
21 Z. J. Huang, J. J. Fu and Y. H. Zhang, *J. Med. Chem.*, 2017, **60**, 7617–7635.
22 D. A. Riccio and M. H. Schoenfisch, *Chem. Soc. Rev.*, 2012, **41**, 3731–3741.
23 W. L. Storm and M. H. Schoenfisch, *ACS Appl. Mater. Interfaces.*, 2013, **5**, 4904–4912.
24 Y. Lu, A. Shah, R. A. Hunter, R. J. Soto and M. H. Schoenfisch, *Acta Biomater.*, 2015, **12**, 62–69.
25 A. Lutzke, J. B. Tapia, M. J. Neufeld and M. M. Reynolds, *ACS Appl. Mater. Interfaces*, 2017, **9**, 2104–2113.
26 C. H. Zhang, T. D. Biggs, N. O. Devarie-Baez, S. M. Shuang, C. Dong and M. Xian, *Chem. Commun.*, 2017, **53**, 11266–11277.
27 H. B. Ji, L. Yan, M. J. R. Ahone and M. H. Schoenfisch, *J. Am. Chem. Soc.*, 2018, **140**, 14178–14184.
28 P.-T. Kao, I. J. Lee, I. Liau and C.-S. Yeh, *Chem. Sci.*, 2017, **8**, 291–297.
29 D. J. Salmon, C. L. T. de Holding, L. Thomas, K. V. Peterson, G. P. Goodman, J. E. Saayedra, A. Srinivasan, K. M. Davies, L. K. Keefer and K. M. Miranda, *Inorg. Chem.*, 2011, **50**, 3262–3270.
30 J. Kim, G. Saravanakumar, H. W. Choi, D. Park and W. J. Kim, *J. Mater. Chem. B*, 2014, **2**, 341–356.
31 X. Zhang, G. Tian, W. Y. Yin, L. M. Wang, X. P. Zheng, L. Yan, J. X. Li, H. R. Su, C. Y. Chen, Z. J. Gu and Y. L. Zhao, *Adv. Funct. Mater.*, 2015, **25**, 3049–3056.
32 H. W. Choi, J. Kim, J. Kim, Y. Kim, H. B. Song, J. H. Kim, K. Kim and W. J. Kim, *ACS Nano*, 2016, **10**, 4199–4208.
33 Y. Wang, X. Y. Huang, Y. Y. Tang, J. H. Zou, P. Wang, Y. W. Zhang, W. L. Si, W. Huang and X. C. Dong, *Chem. Sci.*, 2018, **9**, 8103–8109.
34 Z. Shen, K. He, Z. Ding, M. Zhang, Y. Yu and J. Hu, *Macromolecules*, 2019, **52**, 7668–7677.
35 Y. Duan, Y. Wang, X. Li, G. Zhang, G. Zhang and J. Hu, *Chem. Sci.*, 2020, **11**, 186–194.
36 N. Marino, M. Perez-Lloret, A. R. Blanco, A. Venuta, F. Quaglia and S. Sortino, *J. Mater. Chem. B*, 2016, **4**, 5138–5143.
37 Z. Q. Zhang, J. Y. Wu, Z. H. Shang, C. Wang, J. G. Cheng, X. H. Qian, Y. Xiao, Z. P. Xu and Y. J. Yang, *Anal. Chem.*, 2016, **88**, 7274–7280.
38 D. Afonso, S. Valetti, A. Fraix, C. Bascetta, S. Petralia, S. Conoci, A. Feiler and S. Sortino, *Nanoscale*, 2017, **9**, 13404–13408.
39 H. Okuno, N. Ieda, Y. Hotta, M. Kawaguchi, K. Kimura and H. Nakagawa, *Org. Biomol. Chem.*, 2017, **15**, 2791–2796.
40 H. H. He, Y. X. Liu, Z. N. Zhou, C. L. Guo, H. Y. Wang, Z. Wang, X. L. Wang, Z. Q. Zhang, F. G. Wu, H. L. Wang, D. J. Chen, D. H. Yang, X. W. Liang, J. Q. Chen, S. M. Zhou, X. Liang, X. H. Qian and Y. J. Yang, *Free Radical Biol. Med.*, 2018, **123**, 1–7.
41 C. J. Reinhardt, E. Y. Zhou, M. D. Jorgensen, G. Partipilo and J. Chan, *J. Am. Chem. Soc.*, 2018, **140**, 1011–1018.
42 H. Thomsen, N. Marino, S. Conoci, S. Sortino and M. B. Ericson, *Sci. Rep.*, 2018, **8**, 9753.
43 E. Y. Zhou, H. J. Knox, C. J. Reinhardt, G. Partipilo, M. J. Nilges and J. Chan, *J. Am. Chem. Soc.*, 2018, **140**, 11686–11697.
44 X. Luo, J. Li, J. Zhao, L. Y. Gu, X. H. Qian and Y. J. Yang, *Chin. Chem. Lett.*, 2019, **30**, 839–846.
45 J. H. Park, S. Lee, J. H. Kim, K. Park, K. Kim and I. C. Kwon, *Prog. Polym. Sci.*, 2008, **33**, 113–137.
46 L. Zhang, F. X. Gu, J. M. Chan, A. Z. Wang, R. S. Langer and O. C. Farokhzad, *Clin. Pharmacol. Ther. Ser.*, 2008, **83**, 761–769.
47 R. K. Jain and T. Stylianopoulos, *Nat. Rev. Clin. Oncol.*, 2010, **7**, 653–664.
48 J. J. Shi, A. R. Votruba, O. C. Farokhzad and R. Langer, *Nano Lett.*, 2010, **10**, 3223–3230.
49 N. Bertrand, J. Wu, X. Y. Xu, N. Kamaly and O. C. Farokhzad, *Adv. Drug Delivery Rev.*, 2014, **66**, 2–25.
50 S. Wilhelm, A. J. Tavares, Q. Dai, S. Ohta, J. Audet, H. F. Dvorak and W. C. W. Chan, *Nat. Rev. Mater.*, 2016, **1**, 16014.
51 J. J. Shi, P. W. Kantoff, R. Wooster and O. C. Farokhzad, *Nat. Rev. Cancer*, 2017, **17**, 20–37.
52 L. Schmolz, M. Wallert and S. Lorkowski, *J. Immunol. Methods*, 2017, **449**, 68–70.
53 R. Desikan, R. Griffiths, J. Hancock and S. Neill, *Proc. Natl. Acad. Sci. U. S. A.*, 2002, **99**, 16314–16318.
54 L. E. McQuade and S. J. Lippard, *Curr. Opin. Chem. Biol.*, 2010, **14**, 43–49.
55 X. Zhang, J. F. Du, Z. Guo, J. Yu, Q. Gao, W. Y. Yin, S. Zhu, Z. J. Gu and Y. L. Zhao, *Adv. Sci.*, 2018, **6**, 1801122.
56 Y. Xue, J. Li, G. Yang, Z. Liu, H. Zhou and W. Zhang, *ACS Appl. Mater. Interfaces*, 2019, **11**, 33628–33636.
57 Y. Xue, J. Tian, Z. Liu, J. Chen, M. Wu, Y. Shen and W. Zhang, *Biomacromolecules*, 2019, **20**, 2796–2808.
58 X. Dong, J. Chang and H. Y. Li, *J. Mater. Chem. B*, 2017, **5**, 5240–5250.
59 X. L. Zhang, C. L. Jia, X. Y. Qiao, T. Y. Liu and K. Sun, *Polym. Test.*, 2017, **62**, 88–95.
60 J. Kaplon, L. Zheng, K. Meissl, B. Chaneton, V. A. Selivanov, G. Mackay, S. H. van der Burg, E. M. Verdegaal, M. Cascante,

T. Shlomi, E. Gottlieb and D. S. Peeper, *Nature*, 2013, **498**, 109–112.

61 S. P. Y. Li, C. T. S. Lau, M. W. Louie, Y. W. Lam, S. H. Cheng and K. K. W. Lo, *Biomaterials*, 2013, **34**, 7519–7532.

62 X. Guo, P. Bian, J. Liang, Y. Wang, L. Li, J. Wang, H. Yuan, S. Chen, A. Xu and L. Wu, *Chem. Res. Toxicol.*, 2014, **27**, 990–1001.

63 V. Donato, F. R. Ayala, S. Cogliati, C. Bauman, J. G. Costa, C. Lenini and R. Grau, *Nat. Commun.*, 2017, **8**, 14332.

64 A. G. Charlesworth, U. Seroussi and J. M. Claycomb, *Cell*, 2019, **177**, 1674–1676.

65 Y. L. Chen, J. Tao, P. J. Zhao, W. Tang, J. P. Xu, K. Q. Zhang and C. G. Zou, *Nat. Commun.*, 2019, **10**, 2602.

66 M. Wang, Y. Nie, Y. Liu, H. Dai, J. Wang, B. Si, Z. Yang, L. Cheng, Y. Liu, S. Chen and A. Xu, *Ecotoxicol. Environ. Saf.*, 2019, **170**, 635–643.